MODELLING OF THE MELT POOL BEHAVIOUR DURING A PULSED TIG WELDING OPERATION IN A NARROW GROOVE

S. CADIOU*, A. BAUMARD*, A. BROSSE*, V. BRUYERE**

**Framatome-DTIM, 2 Rue Professeur Jean Bernard, 69007 Lyon, France*
***SIMTEC, 5 rue Félix Poulat, 38000 Grenoble, France*

DOI 10.3217/978-3-85125-968-1-07

ABSTRACT

Arc welding is one of the main processes for assembling metal components in the nuclear industry. To guarantee the quality of the welded assemblies and to predict the characteristics of the weld, it is necessary to master the welding process and have a thorough understanding of the interactions within the melt pool. To this end, the objective of this work is to develop a transient numerical model allowing for the prediction of the behaviour of the melted zone during current pulsation in reasonable computational times. The relevant industrial application in this study is the welding of a narrow groove gap of a stainless steel pipe. The welding process used is pulsed TIG and different synergies are studied. In this work, numerical simulation is used as a predictive analysis tool providing data that complete the experimental ones. Knowing that the predictive aspect of the simulations depends on the modelling choices, it is necessary to consider the main physical phenomena governing the melt pool (thermal transfers, fluid flow, electromagnetism) and to model the mass feeding process using the Arbitrary Lagrangian Eulerian (ALE) method. The development of the magneto-thermohydraulic model with material supply is carried out using the Comsol Multiphysics® software.

Keywords: pulsed TIG welding, groove welding simulation melt pool, magnetohydrodynamics, heat transfer

INTRODUCTION

Framatome's activities in the nuclear industry require a high level of expertise in assembly processes, including welding processes, to ensure that manufactured components respect industrial standards. This accurate knowledge of assembly processes is historically based on empirical approaches, resulting from experimental feedbacks that have demonstrated their capacity in classifying Framatome as one of the leaders in the mastery of welding techniques. Nevertheless, these experimental approaches are expensive and lead to both a limited understanding of the correlation between the operating parameters and the properties of the welds, and of the origin of the defects generated during welding. To reduce experimental costs and improve the comprehension of welding processes,

Framatome has developed numerical tools. Originally, numerical simulation of welding techniques focused on Thermo-Mechanical-Metallurgical (TMM) studies to predict the distortions and residual stresses of the manufactured assembly. Although the power of computational tools has considerably increased during last decades, assumptions are made to simplify the global physical model and thus reduce computational times. Since 2013, Framatome has been developing predictive tools for numerical simulation. These multiphysics models are based on the process parameters (electric current intensity, arc height, shielding gas flow) to simulate a welding operation. The development of these models enables to study the influence of the process parameters on the physical quantities relevant to TIG (Tungsten Inert Gas) (weld pool, electric arc, detachment of the drop from the filler wire or other), to have a better understanding of the phenomenon involved in welding.

Before developing the different aspects of the model, the physics of arc welding processes is explained in a first section. The numerous physical phenomena involved are described, with particular emphasis on the magnetothermo-hydraulic ones. Then, the results from a simplified model of the pulsed TIG welding process with filler metal in a narrow groove, known as Orbital Narrow Gap GTA (Gas Tungsten Arc) welding, are presented in a second section. The model studied here is considered as simplified because the filler metal is not directly modelled but only included in a source term.

MATHEMATICAL FORMULATION AND GOVERNING EQUATIONS

The mathematical description made in this section focuses on the modelling of the melt pool. The plasma, the tungsten electrode used for TIG welding and the filler wire integrating the detachment of the drop are not modelled.

The main purpose of this section is to describe the physical phenomena (Fgi. 1) in a mathematical form, essential to implement the code defining the numerical model. The calculation code used in this study is the COMSOL Multiphysics® software (version 5.6). As a reminder, the physics explained here is related to electromagnetism, heat transfer and fluid mechanics. The ALE method (Arbitary Lagrangian Eulerian) is used to describe the free surface.

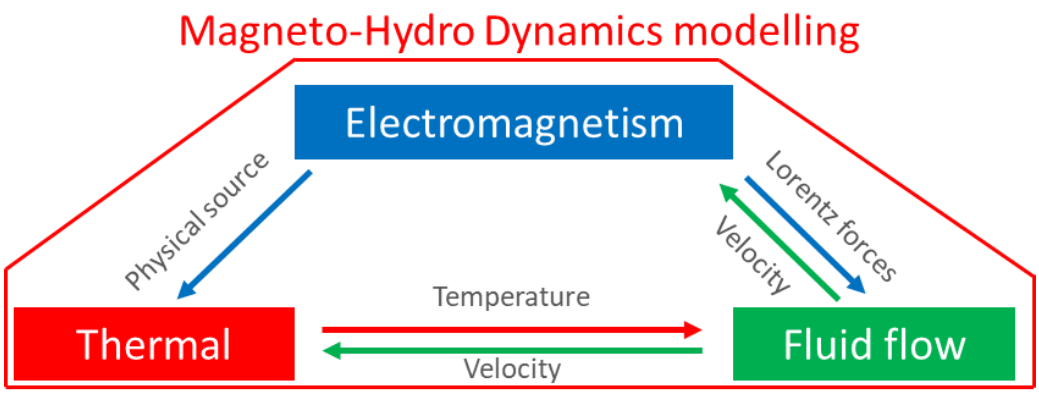

Fig. 1 Multiphysics couplings in the modelling of arc welding

ELECTROMAGNETISM

To determine the electromagnetic forces acting on the flow in the melt pool as well as the Joule effect, the Maxwell equations given below are solved:

$$div\left(\sigma_e \overrightarrow{grad}(V) + \sigma_e \frac{\partial \vec{A}}{\partial t}\right) = 0$$

$$\sigma_e \frac{\partial \vec{A}}{\partial t} + \frac{1}{\mu_0} \overrightarrow{rot}\left(\overrightarrow{rot}(\vec{A})\right) + \sigma_e \overrightarrow{grad}(V) = \vec{0} \quad (1)$$

where σ_e is the electrical conductivity, V is the electrical potential, μ_0 is the magnetic permeability and A is the magnetic vector potential.

THERMAL

The temperature field is calculated using the energy conservation equation:

$$\rho C_p \left(\frac{\partial T}{\partial t} + \vec{v}.\overrightarrow{grad}(T)\right) = div\left(\bar{\bar{k}}\,\overrightarrow{grad}(T)\right) + S_v \quad (2)$$

where ρ is the density, C_p is the specific heat, k is the thermal conductivity, T is the temperature, and S_v a volumetric heat source term. Here, S_v is the heating Joule effect (with j is current density, and E is electric field):

$$S_v = \vec{j}.\vec{E} \quad (3)$$

FLUID FLOW

The flows within the melt pool can be calculated from the conservation equations of mass and momentum:

- Conservation of mass:

$$\frac{\partial \rho}{\partial t} + div(\rho \vec{v}) = 0 \tag{4}$$

where ρ is the density, t the time and $\vec{v}$ the velocity vector.

- Conservation of momentum:

$$\rho\left(\frac{\partial \vec{v}}{\partial t} + \overline{\overline{grad}}(\vec{v}).\vec{v}\right) = \overrightarrow{div}\left[-P\bar{\bar{\imath}} + \mu_f\left(\overline{\overline{grad}}(\vec{v}) + {}^t\overline{\overline{grad}}(\vec{v})\right) - \frac{2}{3}div(\vec{v})\bar{\bar{\imath}}\right] + \overrightarrow{F_v} \tag{5}$$

where P is the pressure, $\bar{\bar{\imath}}$ the identity matrix, μ_f the dynamic viscosity and $\overrightarrow{F_v}$ the volumetric force detailed below.

In the melt pool, the volumetric forces include the electromagnetic forces, also called Lorentz forces, gravity, the buoyancy effect, also called Boussinesq force and a force of extinction of flow velocities called Darcy, allowing to cancel the velocities in the solid part. More specifically, the Boussinesq force is an upward volumetric force caused by changes in the density of a fluid as a function of variations in its temperature and the effects of gravity. It is related to the phenomenon of natural convection. Most of studies use the Boussinesq approximation. It consists in considering that the density varies linearly with the temperature:

$$\vec{F}_v = \vec{F}_{mag} + \vec{F}_b + \vec{F}_{Darcy} + \vec{F}_{gravity} = \vec{j} \times \vec{B} - \rho_{ref}\beta\left(T - T_{ref}\right)\vec{g} - C\frac{(1-f_L)^2}{f_L^3 + b}\vec{v} + \rho\vec{g} \tag{6}$$

where $\vec{F}_{mag}$ represents the electromagnetic forces, $\vec{B}$ the magnetic field, j the electric current density, $\vec{F}_b$ the buoyancy force, $\vec{F}_{Darcy}$ the Darcy law and $\vec{F}_{gravity}$ the gravity. The Darcy law enables to stop the fluid flow in the solid region. ρ_{ref} corresponds to the density at the reference temperature T_{ref}, β to the thermal expansion coefficient, $\vec{g}$ to the acceleration due to gravity, Cd b are two constants and f_L is the liquid fraction function. This function is assumed to vary linearly with temperature in the mushy zone as follows:

$$f_L = \begin{cases} 1 & \text{if } T > T_L \\ \frac{T - T_S}{T_L - T_S} & \text{if } T_S \leq T \leq T_L \\ 0 & \text{if } T < T_S \end{cases} \tag{7}$$

where T is the current temperature, T_S and T_L are the solidus and liquidus temperatures of the workpiece.

INTERFACE EQUATIONS

To model electromagnetism effects, an electric current density is applied using a surfacic Gaussian distribution. The electrical intensity of the process is involved:

$$J_{arc} = d\frac{I_{elec}}{\pi r_0^2}\exp\left(-d\frac{(x-x_0)^2+(y-y_0)^2}{r_0^2}\right) \quad (8)$$

where r_0 is the arc radius, I_{elec} the intensity of the electric current, x_0 and y_0 the coordinates of the centre of the welding torch and d the parameter to be calibrated for the process. In the case of TIG welding with filler metal, d is generally equal to 3 [1].

To describe thermal effects at the interface, additional energy terms are used to modify the energy balance defined as follows:

$$\vec{q}_{total}.(-\vec{n}) = Q_{arc} + s_{radiation} + s_{convection} \quad (9)$$

where $\vec{q}_{total}$ is the total heat flux received by Q_{arc}, $s_{radiation}$, and $s_{convection}$

The description of these terms is given below:

- The heat input generated by the process is assumed to follow a surfacic Gaussian distribution:

$$Q_{arc} = d\frac{\eta_{elec}U_{elec}I_{elec}}{\pi r_0^2}\exp\left(-d\frac{(x-x_0)^2+(y-y_0)^2}{r_0^2}\right) \quad (10)$$

where U_{elec} is the voltage of the electric current and η_{elec} the numerical efficiency applied to the power.

- Radiation losses:

$$s_{radiation} = -\varepsilon\sigma_B(T^4 - T_{amb}^4) \quad (11)$$

where σ_B is the Stefan-Boltzmann constant, ε the emissivity, T the temperature at the surface of the part and T_{amb} is the ambient temperature.

- Convection losses:

$$s_{convection} = -h_c(T - T_{amb}) \quad (12)$$

where h_c is a convective exchange coefficient.

INTERFACE EQUATIONS FOR FLUID FLOW WITH THE FREE INTERFACE (ALE METHOD)

Under the action of the gravitational force, of the arc pressure and of the surface tension acting on the melt pool, the free surface of the molten metal deforms. Even though the amplitude of this deformation is directly related to the welding current and to the arc voltage, it remains relatively low in TIG compared to other welding processes such as MAG, during which the impact of the droplets considerably deforms the free surface [2].

The development of this model is based on the work of Ushio and Wu [3], also taken up by Le Guen [4] and Traidia [2]. It relies on a variational approach which consists in minimizing the total energy of the weld pool and in constraining it to a constant volume, defined by the mass flow rate of filler metal. The energy of the melt pool depends on the variation of the surface energy with the change in the corresponding area (linked to the consideration of the filler metal), on the potential energy due to gravity, and on the work done by arc pressure on the surface. We have designed this approach to predict the deformation of the surface of the weld pool in TIG welding with filler metal using COMSOL Multiphysics® software. The total energy can therefore be expressed according to equation (13).

$$E_{totale} = \iint_S \left(\gamma\left(\sqrt{1+\phi_{|x}^2+\phi_{|y}^2}-1\right)+\frac{1}{2}\rho g\phi^2 - P_{arc}\phi\right)dxdy \quad (13)$$

where S is the upper surface of the part, γ the surface tension, ρ the density of the metal, P_{arc} the arc pressure, ϕ the space function giving, along the vertical axis z, the position of the surface of the melt pool with respect to the undistorted reference plane. The indices |x and |y correspond to the derivatives of the variables concerned with respect to x and y.

The arc pressure is defined by a gaussian distribution of the following form:

$$P_{arc} = dP_{max}\exp\left(-d\frac{(x-x_0)^2+(y-y_0)^2)}{r_0^2}\right) \quad (14)$$

with P_{max} the maximum pressure of the arc which is defined as follows:

$$P_{max} = \frac{\mu_{0_{elec}} I_{elec}^2}{\pi r_0^2} \quad (15)$$

where, as a reminder, r_0 is the arc radius, $\mu_{0_{elec}}$is the magnetic permeability, I_{elec} is the intensity of the electric current, x_0 and y_0 are the coordinates of the centre of the welding torch, and d is the parameter to be calibrated for the process, (generally equal to 3 for TIG process application with filler metal [1]).

The Marangoni force, also known as the surface tension gradient force, is also considered. It is defined by the following equation:

$$\vec{F}_{marangoni} = \frac{\partial\gamma}{\partial T}\overrightarrow{\nabla_S T} \quad (16)$$

where γ is the surface tension defined according to a Sahoo law [5].

RESULTS AND DISCUSSION

EXPERIMENTAL VALIDATION

The development of the model is based on the TG4 model of the NeT network (Neutron Techniques Standardization for Structural Integrity) [6]. The material used is 316L stainless steel. The geometry of the TG4 groove as well as its dimensions are shown in Fig. . To reduce the duration of the calculation, a local adaptation of the mesh is performed (limiting the number of elements) and only the thermal equations are solved on the totality of the geometry. Consequently, fluid mechanics and electromagnetism are treated in a restricted domain encompassing the melt pool and slightly larger than its size. It is in this domain that the mesh is refined. Moreover, the model being symmetrical with respect to the plane (xz), only half of the geometry is modelled (Fig. 2).

Table 1 Welding parameters used for TG4 groove [6]

Intensity	Voltage	Travel speed	Wire feed speed	Wire diameter
220 A	10 V	76.2 mm/min	29.67 mm/s	0.9 mm

The welding parameters used to fill the TG4 groove are presented in Table 1 [6] and are used in the numerical model. As the model does not consider the cycles of variation of the wire feed speed, the average value of this wire speed is chosen for the simulation.

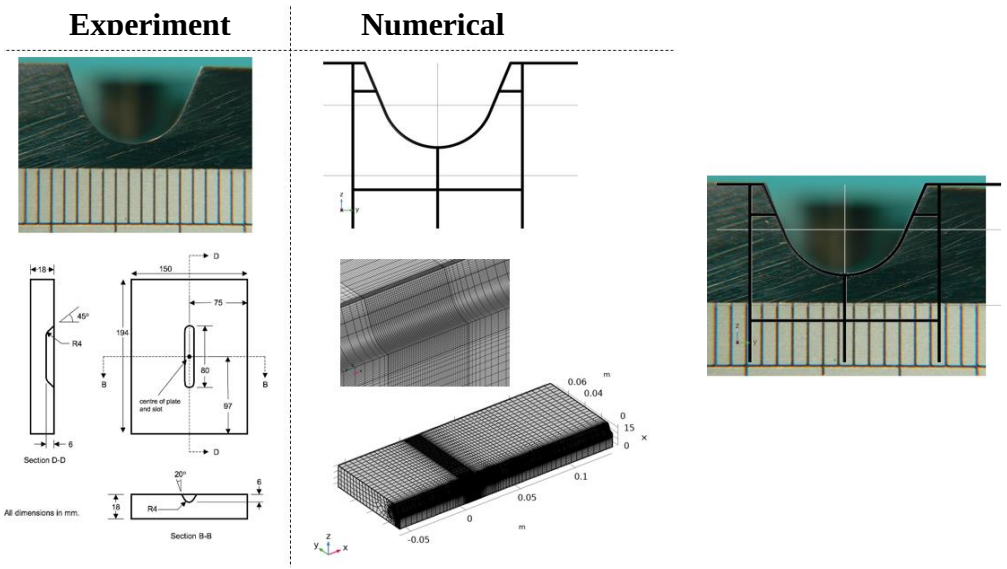

Fig. 2 Experimental and numerical geometries of the TG4 mock-up groove [6]

The results presented below focus on the behaviour of the melt pool. First, one can observe in Fig. 3 the thermal field as well as the shape of the weld pool, highlighted by the purple curve formed by the Iso-value corresponding to the melting temperature (fixed

at 1700 K). Then in Fig. 4 are represented the velocity field and vectors of the fluid flow within the melt pool.

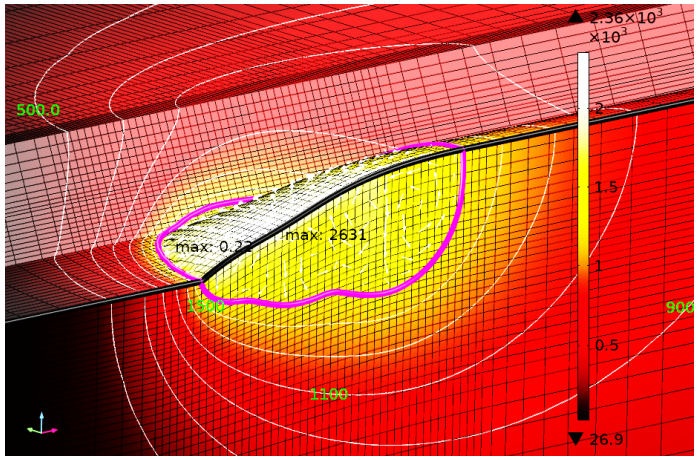

Fig. 3 Temperature field (in K) in the melt pool of the first bead

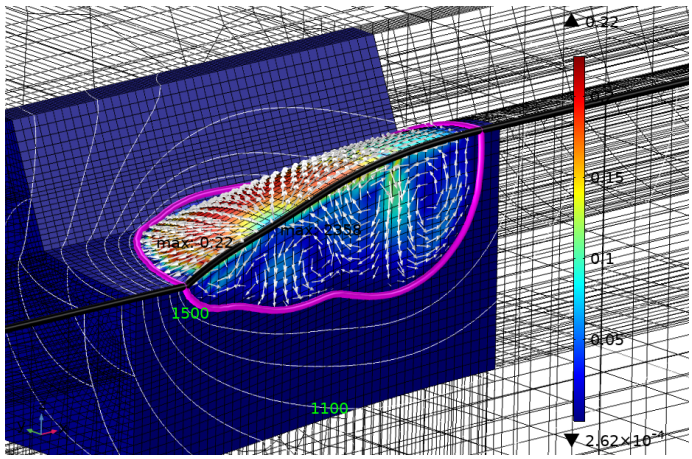

Fig. 4 Velocity field and vectors (in $m.s^{-1}$) of the fluid flow in the melt pool of the first bead

To estimate the validity of the model, comparisons between numerical and experimental results are made. More specifically, are compared:

- Macrographs;
- The thermal evolution obtained by thermocouples.

Fig. 5 shows a good agreement between the melted zones obtained experimentally in the case of the TG4 study (surface in the centre of the figure in light grey) and the melted zones generated by numerical simulation (represented by the purple outline).

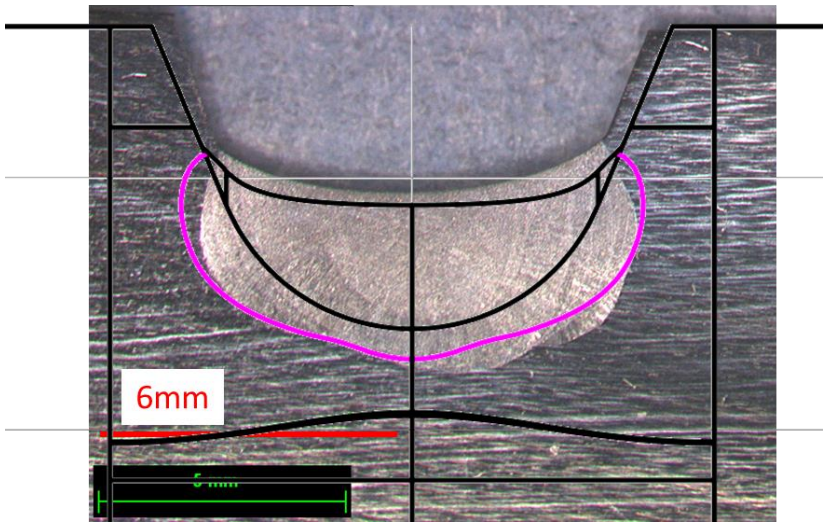

Fig. 5 Comparison of experimental (light grey) and numerical (purple) melted zones

The next step of validation consists in comparing the thermal numerical field to the experimental one. To that purpose, the temperature values recorded by one of the thermocouples of the TG4 study [6] are used as references. This thermocouple is located at the bottom surface of the groove, aligned with the welding direction and centred on the torch position. The numerical model being stationary, it is necessary before to compare simulation results with the thermocouple data, to transform them to obtain a temporal evolution. To this end, temperatures calculated along the central line located below the groove (shown in blue in Fig. 6) are transformed using the ratio of the position along the welding direction (x) and the welding speed:

$$t = \frac{x}{V_s} \tag{17}$$

with x the position along the welding direction and V_s the welding speed.

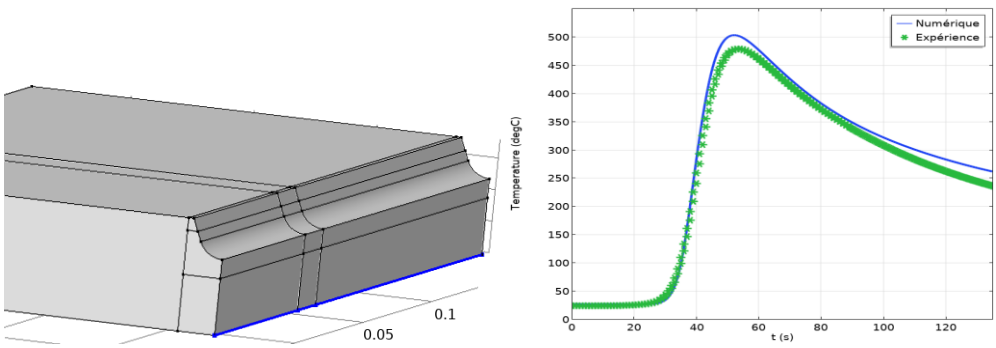

Fig. 6 Representation of the segment used for the comparison of numerical temperatures and temperature measurements recorded experimentally by the thermocouple

Fig. 6 allows for the comparison of the temperature evolution observed experimentally (via the thermocouple) with the one obtained by simulation. Although the model overestimates the maximum temperature (around 20°C), we can notice similar trends.

PULSED TIG MODEL FOR ORBITAL NARROW

The simulation of the TG4 groove leads to the validation of the model. Indeed, the results indicate its ability to predict the geometry of the bead and the thermal field of the part based on the welding parameters.
To consider the cycles of intensity pulsation, it is then necessary to realize a transient model. A first approach would consist in modelling the formation of the bead from its beginning to its steady state. The main advantage of this model is that the shape of the bead can be simulated from the very first moments of welding. The main disadvantage is that it requires the resolution of fluid mechanics equations over a wide area, which leads to significant calculation times (about a month). This first approach should be avoided when dealing with sensitivity studies on process parameters and therefore is inappropriate in the context of this study.

The innovative approach described below enables the integration of the transient aspect of the studied problem, with the advantage of limiting the computational times. It is based on two successive calculations: a stationary calculation identical to the one used in the case of the TG4 model, and a transient magneto-thermohydraulic calculation without filler metal. The first calculation aims at obtaining the established shape of the weld bead from averaged welding parameters, such as the intensity of the electric current. The results obtained at the end of the stationary calculation is then used as initial conditions for the transient calculation. This calculation allows for the simulation of the pulsation cycles of the current intensity and for the study of the consequences of these cycles on the behaviour of the melt pool.

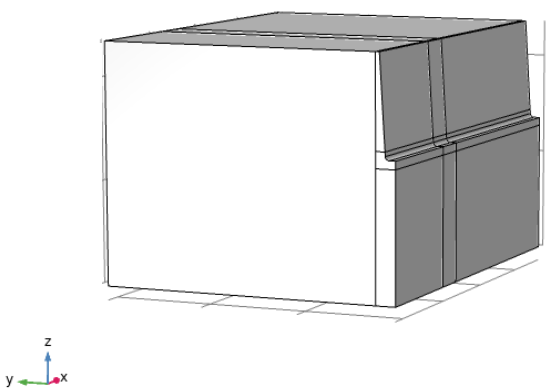

Fig. 7 Geometry of the narrow gap model with a symmetry of the plane (xz)

Considering the shape of the bead obtained during the transient calculation and assuming a negligible deformation of the weld pool during the pulsation cycles, it was

decided not to model the filler metal. As a note, less than 4 days are needed to simulate 4 seconds of physical time (*i.e.*, real welding time), since the duration of the calculation is around 10 hours for the stationary model and varies from 24 to 72 hours for the transient model. The dimensions of the orbital narrow gap model are confidential. Nevertheless, the geometry of the groove is presented in Fig. 7. The material used is of stainless-steel type. The process parameters used to develop the model are confidential Framatome data.

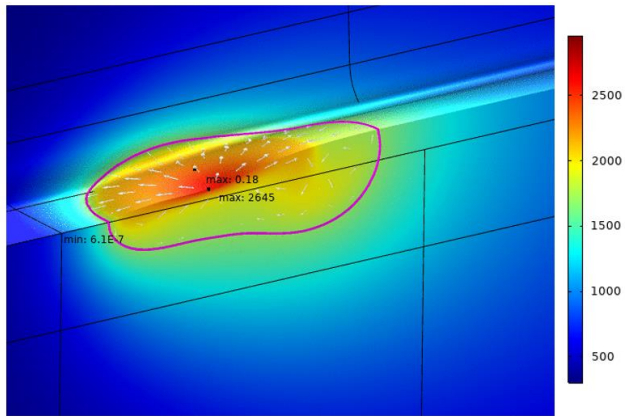

Fig. 8 Thermal field (in K) and velocity vectors of the fluid flow within the melt pool. The purple curve corresponds to the melting isovalue (1700 K).

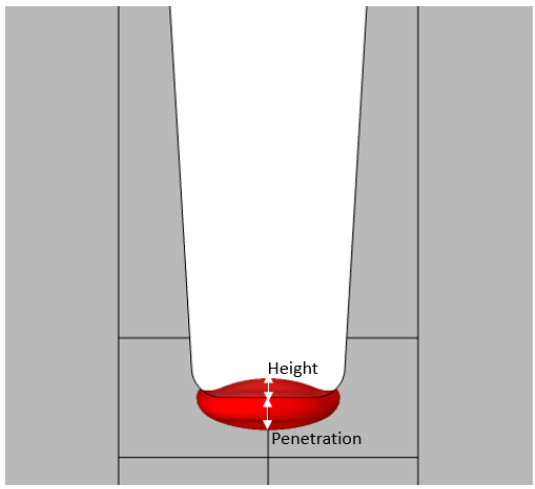

Fig. 9 Numerical macrograph with the melted zone represented in red (temperature above 1700 K)

Fig. 8 and Fig. 9 summarize the simulation results. Fig. 9 shows the thermal field and the fluid flow velocity vectors within the weld pool. The shape of the melt pool is

represented by the purple curve generated by the fusion isovalue (temperature of 1700 K). Fig. 9, corresponds to the numerical macrograph simulated.

The results from the transient calculation describe the variations in shape of the melt pool during the intensity pulsation cycles. Fig. 10, Fig. 12, Fig. 13 and Fig. 14 show, as a function of intensity, the variations in elongation, width, penetration, and volume of the weld pool respectively. In these figures are plotted:

- Continuous lines: representing the characteristic pool dimensions;
- Dashed lines: depicting the current intensities;
- Dotted lines: corresponding to the slope of the speed of the welding torch (only Fig. 10).

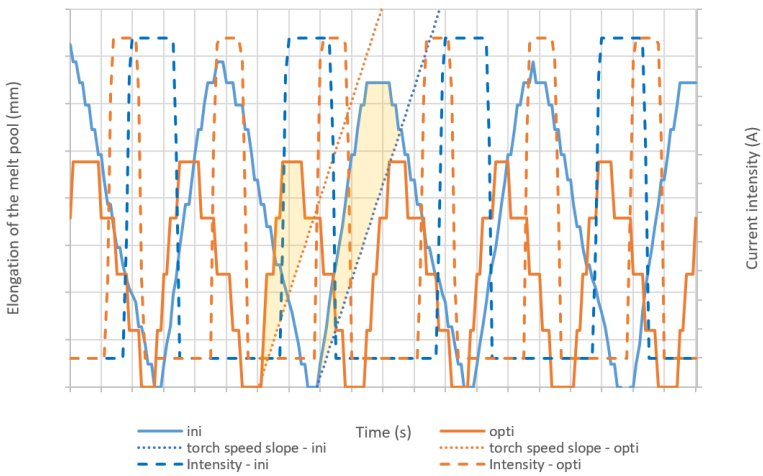

Fig. 10 Evolution of the elongation of the melt pool during the intensity pulsation cycles using the initial (blue curves) and optimized (orange curves) process parameters

Two different sets of parameters are tested within the framework of this study: an initial one and an “optimized” one that leads to the obtention of a more stable weld pool. During stationary simulations the power is determined by averaging the parameters related to the electric current (intensity and voltage). In the present case, the two sets of parameters, “initial” and “optimized”, give the same average power, which would lead to identical results for a stationary simulation. Therefore, it is important to define a transient model to be able to perform an accurate analysis of the behaviour of the melt pool. In the following, the results of simulations carried out with the initial set of parameters are identified by the blue curves and those related to the optimized set of parameters by the orange curves.

Comparing the curve of the welding torch speed of advance and the elongation of the melt pool (Fig. 10, Fig. 11), one can observe that the pool grows faster than it moves. Indeed, the two areas represented in yellow in the figure located above the dotted lines (slope of the speed of the torch), and under the continuous lines show that the pool grows faster than the torch moves. The weld bead therefore undergoes a remelting during

electric current intensity pulsations. Intensity pulsation cycles also highlight the disadvantage of using stationary calculations.

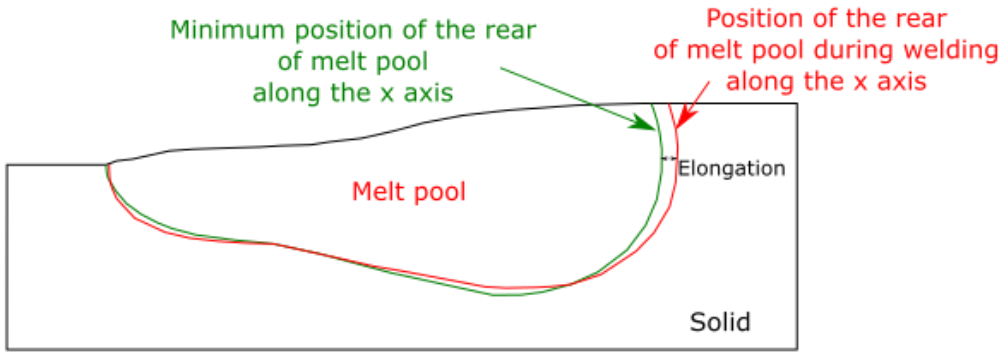

Fig. 11 Diagram representing the elongation of the melt pool

The results obtained being confidential, only the analysis of the relative deviations, $\varepsilon_{difference}$ is made:

$$\varepsilon_{difference} = \frac{variation_{opti} - variation_{ini}}{variation_{ini}} \quad (18)$$

Table 2 summarizes the relative deviations obtained for the various observables, namely the elongation of the melt pool, its width, its penetration, its volume, its maximum temperature and its maximum flow velocity. This table shows that intensity pulsation cycles have a significant impact on the shape of the melt pool. Indeed, the table highlights the fact that the weld pool undergoes less significant variations during a pulsation cycle with the optimized parameters than with the initial parameters, since these variations are reduced by 48% if we focus on the volume of the weld pool. Fig. 12, Fig. 13 and Fig. 14 reinforce the conclusions of Table 2.

Table 2 Relative deviations of the variations of the different observables

Observables	Relative deviation of the variations between initial and optimized parameters
Elongation of the tail of the weld pool	-28 %
Width	-26 %
Penetration	-3 %
Volume	-48 %
Maximum temperature	-4,56 %
Maximum fluid flow velocity	-5,71 %

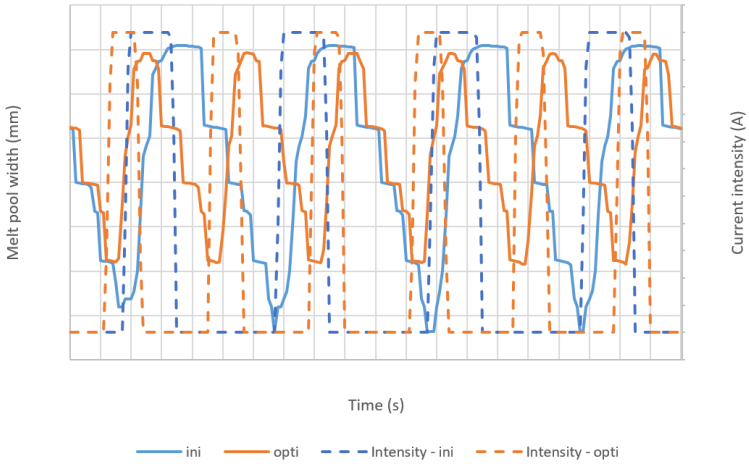

Fig. 12 Evolution of the width of the melt pool during cycles of intensity pulsation for the initial (blue curves) and optimized (orange curves) parameters

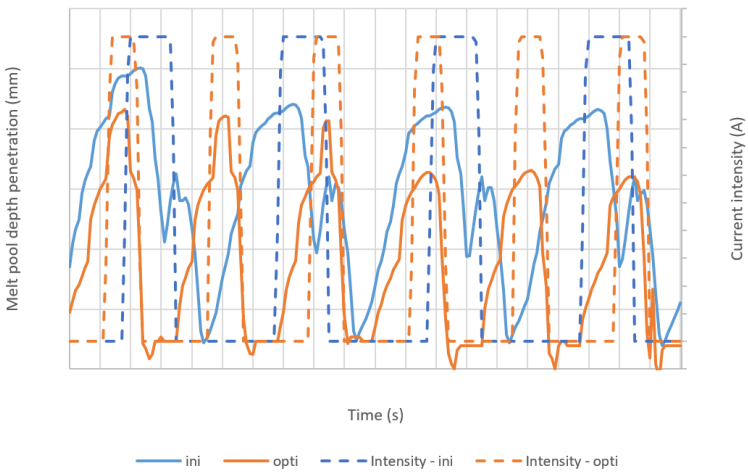

Fig. 13 Evolution of the melt pool depth penetration during intensity pulsation cycles for initial (blue curves) and optimized (orange curves) parameters

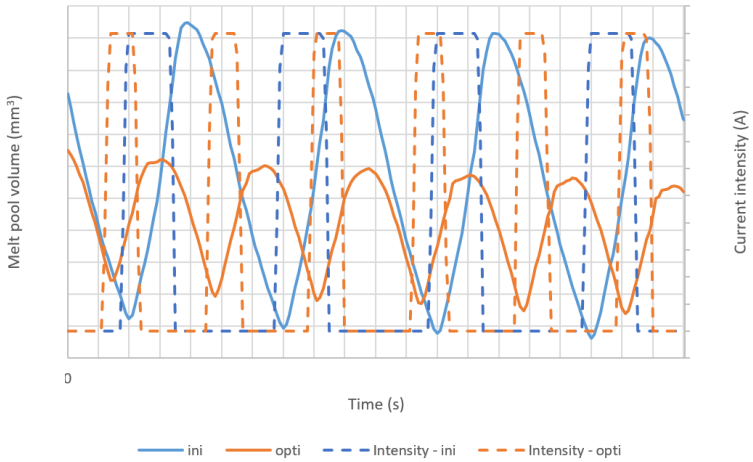

Fig. 14 Evolution of the melt pool volume during intensity pulsation cycles for initial (blue curves) and optimized (orange curves) parameters

CONCLUSION

This paper presents some of the work carried out by Framatome in the modelling of the melt pool formed by welding processes aiming at the contribution of the improvement of the control of these processes.

Framatome being interested in the welds used in the nuclear industry, the objective of this study was to develop a model suitable for industrial configurations of the Orbital Narrow Gap GTA Welding type to improve the understanding of the influence of the operating parameters on the behaviour of the weld pool. First step consisted in developing a model consistent with the physics of the weld pool, based on experimental data. A model already used by Framatome was chosen, including a narrow chamfer. After comparing the experimental and numerical temperatures and weld pool shapes, a good agreement was found, allowing for the validation of the defined simulation method for a typical welding configuration.

The methodology was then specially adapted to Orbital Narrow Gap GTA Welding processes, which use a pulsed transfer mode. To this end, in addition to the initial stationary model, a transient magneto-thermohydraulic model considering the cycles of pulsations was developed. Finally, the developed approach offers promising results in reasonable computation times.

References

[1] F. HEJRIPOUR, D. T. VALENTINE AND D. K. AIDUN: 'Study of mass transport in cold wire deposition for Wire Arc Additive Manufacturing', *International Journal of Heat and Mass Transfer*, no. 0017-9310 DOI: 10.1016/j.ijheatmasstransfer.2018.04.092, 2018.

[2] A. TRAIDIA: *Multiphysics modelling and numerical simulation of GTA weld pools*, PhD Thesis, Ecole Polytechnique, 2011.

[3] M. USHIO and C. WU: 'Mathematical modeling of three-dimensional heat and fluid flow in a moving gas metal arc weld pool', *Metallurgical and Materials Transactions B-Process Metallurgy and Materials Processing Science*, no. 28:509-516, 1997.
[4] E. LE GUEN, M. CARIN, R. FABBRO, F. COSTE and P. LE MASSON: '3D heat transfer model of hybrid laser Nd :Yag-MAG welding of S355 steel and experimental validation', *International Journal of Heat and Mass Transfer*, vol. 54, p. 1313-1322, 2011.
[5] P. SAHOO, T. DEBROY and M. MCNALLAN: 'Surface tension of binary metal-surface active solute systems under conditions relevant to welding metallurgy', *Metall Mater Trans B*, vol. 19, p. 483-491, 1988.
[6] M. C. SMITH and A. C. SMITH: *2009-09-29_TG4_simulation_protocol*, 2009.
[7] C. S. WU, P. C. ZHAO and Y. M. ZHANG: 'Numerical simulation of transient', *Welding journal*, 83(12):330s-335s, 2004.